Ginaton injection alleviates cisplatin-induced renal interstitial fibrosis in rats via inhibition of apoptosis through regulation of the p38MAPK/TGF-β1 and p38MAPK/HIF-1α pathways

TAOLIN LIANG[1*], CHONGYING WEI[1*], SISI LU[1], MENGYUAN QIN[1], GUIMING QIN[1], YANSONG ZHANG[1], XIAOBIN ZHONG[2], XIAOQIN ZOU[3] and YUFANG YANG[3]

[1]Postgraduate Department of Pharmacy, The First Affiliated Hospital of Guangxi Medical University; [2]Regenerative Medicine Research Center of Guangxi Medical University; [3]Department of Pharmacy, The First Affiliated Hospital of Guangxi Medical University, Nanning, Guangxi 530021, P.R. China

Received October 22, 2020; Accepted February 4, 2021

DOI: 10.3892/br.2021.1414

Abstract. Ginaton injection (Ginkgo biloba extract; GBE) has been reported to protect against cisplatin-induced acute renal failure in rats. In the present study, the effects and molecular mechanisms of GBE on cisplatin-induced renal interstitial fibrosis were evaluated using a rat model. The rats were intraperitoneally injected with cisplatin once on the first day and a subset of rats were treated with GBE or SB203580 (SB; a specific p38 MAPK inhibitor) daily from days 22 to 40. The levels of N-acetyl-β-D-Glucosaminidase (NAG) in the urine, and of urea nitrogen (BUN) and creatinine (Scr) in the blood were assessed. The damage and fibrosis of renal tissues were evaluated using hematoxylin and eosin staining, as well as Masson's trichrome staining, respectively. Apoptosis in renal tissues was detected using a TUNEL assay. The protein expression levels of α-smooth muscle actin (SMA), collagen 1 (Col I), Bax, Bcl-2, caspase-3/cleaved caspase-3, hypoxia-inducible factor-1α (HIF-1α), TGF-β1 and p38MAPK, as well as the mRNA levels of p38MAPK in renal tissues were investigated. The results showed that GBE markedly reduced the levels of urinary NAG, Scr and BUN, and renal expression of α-SMA and Col I levels were also reduced. Furthermore, GBE significantly reduced renal tissue injury and the relative area of renal interstitial fibrosis induced by cisplatin. GBE effectively reduced the apoptotic rate of renal tissues, the protein expression levels of Bax, cleaved caspase-3, phospho-p38MAPK, TGF-β1 and HIF-1α, as well as the mRNA expression levels of p38MAPK in renal tissues induced by cisplatin, whereas GBE significantly increased Bcl-2 protein expression. SB exhibited similar effects to GBE, although it was not as effective. In summary, the present study is the first to show that GBE significantly alleviated renal interstitial fibrosis following cisplatin-induced acute renal injury. The mechanisms by which GBE exhibited its effects were associated with the inhibition of apoptosis via downregulation of the p38MAPK/TGF-β1 and p38MAPK/HIF-1α signaling pathways.

Correspondence to: Professor Xiaobin Zhong, Regenerative Medicine Research Center of Guangxi Medical University, 6 Shuangyong Road, Qingxiu, Nanning, Guangxi 530021, P.R. China
E-mail: 1878125675@qq.com

Professor Yufang Yang, Department of Pharmacy, The First Affiliated Hospital of Guangxi Medical University, 6 Shuangyong Road, Qingxiu, Nanning, Guangxi 530021, P.R. China
E-mail: 814896670@qq.com

*Contributed equally

Key words: ginaton injection, cisplatin-induced renal interstitial fibrosis, apoptosis, p38MAPK, hypoxia-inducible factor-1α

Introduction

Cisplatin remains the primary and most frequently used chemotherapeutic option for the management of solid tumors (1). However, cisplatin, even at commonly used doses, may induce acute renal injury to varying degrees, and this may affect the continuous administration of chemotherapy and thus, the prognosis of patients. If left untreated, acute kidney damage can lead to renal interstitial fibrosis and, in severe cases, renal failure (2).

The renal tubular area is the key area affected by acute kidney injury (AKI) caused by cisplatin that eventually develops into interstitial fibrosis (3), and renal interstitial fibrosis is considered to be a key factor underlying chronic renal failure (4). However, the mechanism underlying renal interstitial fibrosis following acute renal injury induced by cisplatin has not been fully elucidated, and there is still a lack of effective preventative and curative measures.

Inflammatory injury, oxidative stress injury and apoptosis are the primary mechanisms of cisplatin-induced kidney injury (5,6), and hypoxia is hypothesized to be a common feature of all types of AKI (7). Cisplatin has been reported to induce renal cell damage by upregulating the phosphorylation of p38MAPK (8,9). Additionally, hypoxia-inducible factor (HIF)-1α levels are significantly increased in rats

with cisplatin-induced acute kidney damage, which, in-turn protects against renal injury (10,11). However, the roles of p38MAPK and HIF-1α, and their association with apoptosis in renal interstitial fibrosis following cisplatin-induced acute renal injury have not been previously reported, to the best of our knowledge.

Ginaton injection is derived from ginkgo biloba leaves (GBE) and has been used for several decades for the treatment of cardiovascular and cerebrovascular diseases (12,13). Previous reports have shown that GBE can prevent testicular injury via its anti-apoptotic and anti-inflammatory effects (14), reducing H_2O_2-induced cell cytotoxicity via downregulation of p38 MAPK (15), and can also inhibit the hepatic fibrosis and attenuate brain death-induced renal injury by reducing the activity of p38MAPK (16,17). Additionally, GBE can inhibit the growth of transplanted solid tumors in mice, and dose-dependently reduce the protein and mRNA expression levels of HIF-1α (18). Our previous study showed that GBE can protect against cisplatin-induced acute renal injury, and thus the subsequent renal interstitial fibrosis (19). However, whether GBE can reduce renal interstitial fibrosis following cisplatin-induced acute renal injury, and the mechanisms underlying its effects, remain to be determined. In the present study, the effects of GBE were assessed on renal interstitial fibrosis following cisplatin-induced acute renal injury via detection of apoptosis, and based on the expression of p38MAPK, TGF-β1 and HIF-1α during this process.

Materials and methods

Drugs and antibodies. GBE injection (batch number IB122) was purchased from Dr Willmar Schwabe Pharmaceuticals. Each 17.5 mg ampule of GBE consisted of 24% Ginkgo flavonol glycosides and 6% terpene lactones. Cisplatin power injection (batch no. 5050272DB) was provided by Qilu Pharmaceutical Co., Ltd. The anti-α-smooth muscle actin (SMA) (cat. no. BM0002), anti-collagen 1 (Col I) (cat. no. BA0325), anti-p38MAPK (cat. no. 9215S), anti phospho-(p-)p38MAPK (cat. no. 8690S), anti-TGF-β1 (cat. no. ab179695), anti-HIF-1α (cat. no BS-3514) and anti-β-actin (cat. no. 3700S) antibodies were purchased from Cell Signaling Technology, Inc. Antibodies against Bcl-2 (cat. no. BM4985), caspase-3 (cat. no. BM4620) and Bax (cat. no. BM3964) were obtained from Wuhan Boster Biological Technology, Ltd.

Animals. Male Sprague-Dawley rats (body weight, 200±20 g) were purchased from the Experimental Animal Center of Guangxi Medical University, and were bred in an air-conditioned room where the relative humidity was 60±10% at 25±2˚C, with a 12-h light/dark cycle and *ad libitum* access to food and water. The present study was approved by the Ethics Committee of Guangxi Medical University (approval no. 201310009).

Experimental design. Rats were randomly divided into 5 groups following a 1-week acclimation period (n=9 per group). The rats were grouped as follows: i) Control group, on day 1, rats received saline equal to the volume of cisplatin, and equal to the volume of GBE from days 22 to 40; ii) CDDP group, rats received saline equivalent to the volume of GBE, once a day from days 22 to 40; iii) CDDP + GBE group, rats received GBE (3.17 mg/kg) once a day from days 22 to 40; iv) CDDP + SB203580 (SB; a specific p38 MAPK inhibitor) group, rats received SB (1 mg/kg) once a week from days 22 to 40, and saline equivalent to the volume of GBE once a day (on days where no SB was administered); and v) CDDP + Enalapril group, rats received enalapril (10 mg/kg) once a day from days 22 to 40.

Additionally, the rats in groups ii) to v) were treated with a single dose of cisplatin (5 mg/kg) on day 1 to induce AKI, which developed into renal interstitial fibrosis, as described previously (10,11). Cisplatin, GBE and SB were administered via intraperitoneal injection, whereas enalapril was administered by gavage.

According to the drug dose conversion formulas of different species of animals in China's pharmacological experimental methodology (20), the dose of EGB in this study was converted from the clinically commonly used adult dose to the rat dose, and was also based on the results of the preliminary experiments (data not shown). Enalapril exhibits antioxidant effects and alleviates renal fibrosis (21,22), and these effects are similar to those of GBE (23,24), and is has been used as a positive control drug in an anti-fibrotic study previously (25), thus enalapril was used as a positive control in the present study as well.

Blood, urine and renal tissue collection. On the 40th day, 12 h after administration of the final dose, urine, blood and kidneys were collected and stored at -80˚C. First, urine from each rat was gathered separately. Next, the rats were anesthetized by intraperitoneal injection of sodium pentobarbital (30 mg/kg, ip). When rats were under deep anesthesia (the limbs and abdominal muscles became relaxed, breathing became slow, and the corneal reflex was absent), blood samples were collected from the abdominal aorta and centrifuged at 4˚C for 15 min at 1,409 x g. Finally, exsanguination was performed to euthanize the animals, and when no reflexes and no breathing was observed, the renal samples were obtained and washed using ice-cold saline. A portion of these renal specimens were fixed at room temperature using buffered formalin (10%) for 24 h, and then TUNEL staining, Masson's trichrome staining, hematoxylin and eosin (H&E) staining and immunohistochemistry were performed as soon as possible. The remainder of the renal specimens were immediately refrigerated at -80˚C for western blotting and reverse transcription-quantitative (RT-q)PCR.

Determination of blood urea nitrogen (BUN), serum creatinine (Scr) and urinary N-acetyl-β-D-glucosaminidase (NAG) levels. The levels of NAG (cat no. A031) in the urine were determined using the nitrophenol colorimetric method, and the levels of BUN (cat. no. C013-2) and Scr (cat. no. C011-1) in the peripheral blood were detected using a 7100 automatic biochemical analyzer (Hitachi, Ltd.) using specific kits purchased from Nanjing Jiancheng Bioengineering Research Institute. All procedures were performed strictly in accordance with the manufacturer's protocol (Nanjing Jiancheng Bioengineering Institute).

Hematoxylin and eosin (H&E) staining. Kidney tissues were fixed (as described above) and routinely embedded in paraffin. Next, the kidney tissues were sectioned into 3-4 μm thick slices and then stained with H&E according to the manufacturer's

protocol (Lot no. 0904A18, Beijing Leagene Biotech. Co., Ltd.). Slices were dewaxed with xylene, hydrated using a decreasing gradient of ethanol solutions, and then stained with hematoxylin staining solution for 15 min at room temperature, differentiated using the differentiation solution for 30 sec, stained with the eosin staining solution for 2 min at room temperature, and finally sealed with neutral gum after dehydration using an increasing gradient of ethanol solutions, and clearing using xylene. The stained slices were examined using a light microscope (IX51; Olympus Corporation; magnification, x200). In each sample evaluated, five randomly selected fields of view were assessed and the average score of tubule interstitial injury was calculated. The scoring criteria were based on a previous study (26): 0, normal; 1, cortical damage ≤25%; 2, cortical damage 25-50%; 3, cortical damage 50-75%; and 4, cortical damage >75%. Histopathological changes were scored by an experienced pathologist who was blinded to the conditions of the study.

Masson's trichrome staining. To evaluate renal interstitial fibrosis, the fixed renal sections were stained using a Masson's trichrome staining kit (Lot no. 0215A16, Beijing Leagene Biotech. Co., Ltd). Sections were dewaxed and hydrated as above, then stained at room temperature using a Weigert ferryhematoxylin staining solution for 8 min, Lichunred fuchsin staining solution for 5 min, washed with phosphomolybdate solution for 2 min, and finally, stained with aniline blue staining solution for 2 min. Each renal section was evaluated in five randomly selected non-overlapping visual fields (magnification, x400). The relative area of interstitial fibrosis was measured using the Colour Image Analyser function of Image-Pro Plus version 6.0 (Media Cybernetics, Inc.). The areas overlaying the tubular basement membrane and interstitial space were evaluated, whereas the glomeruli and large vessels were not included in the analysis.

Immunohistochemical detection of renal α-SMA, Col I, TGF-β1 and HIF-1α protein expression. The protein expression levels of α-SMA, Col I, TGF-β1 and HIF-1α in renal tissues were detected using immunohistochemical staining. Briefly, paraffin-embedded renal specimens were cut into slices. After dewaxing with xylene and dehydrating with a gradient of increasing ethanol solutions (95% ethanol followed by anhydrous ethanol 3 times, 5-10 sec each time), the renal slices were incubated in hydrogen peroxide solution (0.3%, 37˚C, 10 min) to quench the endogenous peroxidase activity, followed by incubation at room temperature for 20 min with 10% goat serum for blocking non-specific binding. Next, the corresponding primary antibody was added and incubated with the renal sections (4˚C, overnight). The primary antibodies used were: α-SMA (1:6,000; cat. no. BM0002; Cell Signaling Technology, Inc.), Col I (1:1,400; cat. no. BA0325; Cell Signaling Technology, Inc.), TGF-β1 (1:6,000; cat. no. ab179695; Cell Signaling Technology, Inc.) and HIF-1α (1:1,000; cat. no. BS-3514; Novus Biologicals, LLC). After incubation at 37˚C for 1 h with the secondary antibody diluted in PBS (1:100; cat. no. WP151228; Beijing Zhongshan Jinqiao Biotechnology Co., Ltd), the renal sections were treated with DAB (Wuhan Boster Biological Technology, Ltd.) to develop the signal. Finally, renal slices were visualized using Olympus Soft Imaging Solutions. The sections were observed using a light microscope (IX51; Olympus Corporation). The integrated optical density (IOD) was used to quantify the positively stained area in Image Pro-Plus. The average value of 5 randomly selected fields of view (magnification, x400) for each renal sample was calculated. The protein levels of α-SMA, Col I, TGF-β1 and HIF-1α in renal tissues are expressed as the ratio of IOD to the positive staining area.

TUNEL staining. The paraffin-embedded renal tissues were cut into slices (4 μm). Next, the slices were stained using a TUNEL Apoptosis Detection kit I, POD, according to the manufacturer's protocol (Wuhan Boster Biological Technology, Ltd.). Finally, 5 non-overlapping fields of view of the tubules per renal section were randomly selected using a light microscope (magnification, x400), and the number of positive cells were counted. TUNEL-positive cells showed brown staining in the nucleus, indicative of apoptotic cells. The apoptotic rate (%) was calculated by counting the proportion of positive cells in the total number of cells using Image Pro-Plus.

Western blotting. Kidney tissues of rats were lysed into homogenate with an appropriate amount of tissue Lysis Buffer and liquid nitrogen, and the protein concentration of the lysates was measured using a BCA protein assay kit. Next, equal amounts of protein lysates (100 μg) were separated by 12% SDS-PAGE at 100 V for 2 h, and transferred to PVDF membranes (EMD Millipore) at 4˚C (100 V, 1.5 h). After blocking using Quick Block™ Buffer (Beyotime Institute of Biotechnology) for 15 min at room temperature, the membranes were incubated overnight at 4˚C with the primary antibodies. The primary antibodies included the following: Anti-Bax (1:200; cat. no. BM3964; Wuhan Boster Biological Technology, Ltd.), anti-Bcl-2 (1:200; cat. no. BM4985; Wuhan Boster Biological Technology, Ltd.), anti-caspase-3 (1:200; cat. no. BM4620; Wuhan Boster Biological Technology, Ltd.), anti-p38MAPK (1:500; cat. no. 9215S; Cell Signaling Technology, Inc.) and anti-p-p38MAPK (1:1,000; cat. no. 8690S; Cell Signaling Technology, Inc.). β-actin (1:10,000; cat. no. 3700S, Cell Signaling Technology, Inc.) was used as the internal control. Finally, the membranes were incubated for 1 h with secondary antibody (fluorescent goat anti-rabbit antibody; 1:10,000; cat. no. 5151S; Cell Signaling Technology, Inc.) and signals were visualized using a near-infrared bicolor fluorescence imaging system (Odyssey CLx; Li-COR Biosciences). Densitometry analysis was performed using ImageJ2x (National Institutes of Health).

RT-qPCR. The samples of renal tissues stored at -80˚C were grounded in homogenate with liquid nitrogen to extract RNA. AxyPrep™ Multisource Total RNA Miniprep kit (Axygen; Corning, Inc.) was used to extract total RNA, and then the gDNA Eraser (Takara Bio, Inc.) and the Prime Script™ RT reagent kit were used to reverse transcribe 1 μg total RNA, according to the manufacturer's protocol. qPCR was used to detect the expression levels of target genes using a SYBR® Premix Ex Taq™ II kit (Takara Bio, Inc.) and an Applied Biosystems 7500 Real-Time PCR system (Applied Biosystems; Thermo Fisher Scientific, Inc.). The PCR reaction mix (10 μl) consisted of SYBR Premix Ex Taq II, forward primer (0.5 μl), reverse primer (0.5 μl), ROX Reference DyeII (50x), cDNA (2 μl) and RNase free dH_2O (2 μl). The thermocycling conditions were:

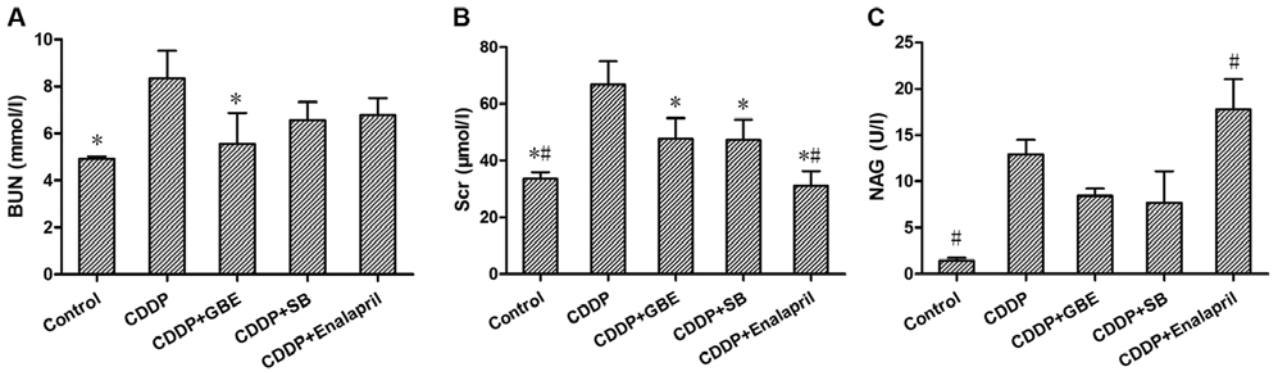

Figure 1. Effects of GBE on renal function in rats with cisplatin-induced renal fibrosis. Concentrations of (A) BUN, (B) Scr, (C) NAG in rats were detected. Data are presented as the mean ± standard deviation. n=9. *P<0.05 vs. CDDP group, #P<0.05 vs. CDDP + GBE group. BUN, blood urea nitrogen; Scr, serum creatinine; NAG, urinary N-acetyl-β-D-glucosaminidase; GBE, Ginkgo biloba extract; SB, SB203580.

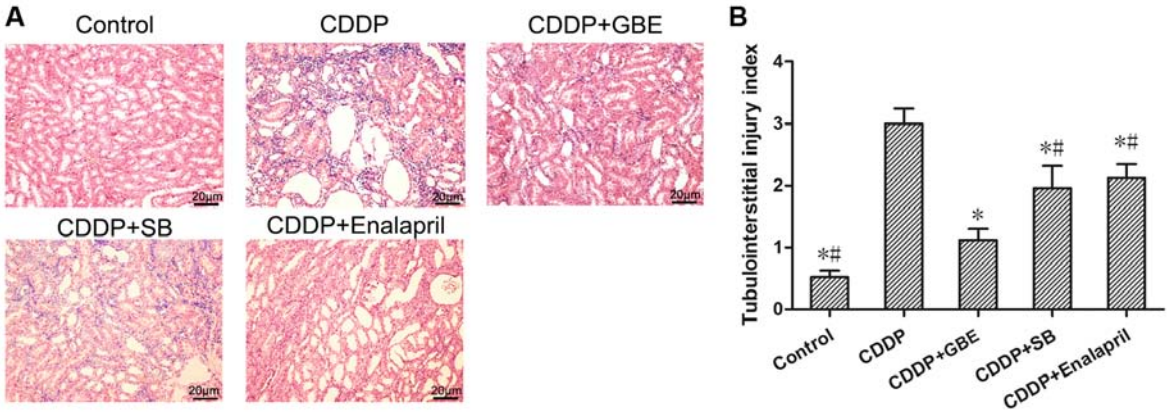

Figure 2. Effects of GBE on the histopathological changes of rat kidney were analyzed using H&E staining. (A) Representative images of H&E stained renal samples. Magnification, x200. The differences in renal tubular lumens stenosis, edema, degeneration and necrosis of tubular epithelial cells were observed using light microscopy. (B) Quantitative analysis of tubulointerstitial injury index. Data are presented as the mean ± standard deviation. n=9. *P<0.05 vs. CDDP group, #P<0.05 vs. CDDP + GBE group. H&E, hematoxylin and eosin; GBE, Ginkgo biloba extract; SB, SB203580.

Denaturation at 95˚C for 30 sec; followed by 40 cycles of 5 sec at 95˚C and 60˚C for 34 sec. The sequences of the primers were: p38MAPK forward, 5'-TTACCGATGACCACGTTC AGTTTC-3' and reverse, 5'-AGCGAGGTTGCTGGGCTT TA-3'; and GAPDH forward, 5'-GGCACAGTCAAGGCT GAGAATG-3' and reverse, 5'-ATGGTGGTGAAGACGCCA GTA-3'. The levels of p38MAPK gene were normalized to that of GAPDH using the $2^{-\Delta\Delta Cq}$ method: $\Delta\Delta Cq=(Cq_{control}-Cq_{treatment})$ reference-$(Cq_{control}-Cq_{treatment})$ target (27).

Statistical analysis. Data are presented as the mean ± standard deviation. SPSS 24.0 (IBM Corp.) was used for statistical analysis. The differences between multiple groups were assessed using a one-way ANOVA with a post-hoc Tukey's test. P<0.05 was considered to indicate a statistically significant difference.

Results

Effect of GBE on kidney function in rats treated with cisplatin. As shown in Fig. 1, cisplatin induced damage to renal function and increased the levels of BUN, Scr and urinary NAG significantly (P<0.05). GBE treatment significantly decreased the cisplatin-induced increase in the levels of BUN and Scr (P<0.05), and there was no significant difference in the NAG levels (P>0.05). SB treatment significantly lowered Scr levels (P<0.05), but had no significant effect on BUN and NAG levels (P>0.05). Enalapril treatment significantly reduced Scr levels, but increased NAG levels (P<0.05). No significant differences were observed in Scr, BUN and NAG levels between the GBE treatment and SB treatment (P>0.05; Fig. 1B and C).

Effect of GBE on renal tissue damage induced by cisplatin. H&E staining showed that there were no histopathological changes in the control rats. Cisplatin treatment resulted in renal tubular lumen stenosis, and a portion of the tubular epithelial cells exhibited signs of oedema, degeneration or necrosis. Conversely, the GBE treatment alleviated renal injury induced by cisplatin, as did the enalapril and SB treatments (P<0.05; Fig. 2A).

The tubular injury score was significantly higher in the CDDP group compared with the Control group (P<0.05). The increased tubular injury score induced by cisplatin was significantly reduced following GBE, SB or enalapril treatment (P<0.05). Additionally, GBE treated rats exhibited significantly lower tubule injury scores compared with the rats treated with SB or enalapril (P<0.05; Fig. 2B).

Masson's trichrome staining showed there was no apparent renal fibrogenesis in the control rats, whereas cisplatin treatment resulted in severe renal interstitial fibrosis (Fig. 3). Cisplatin

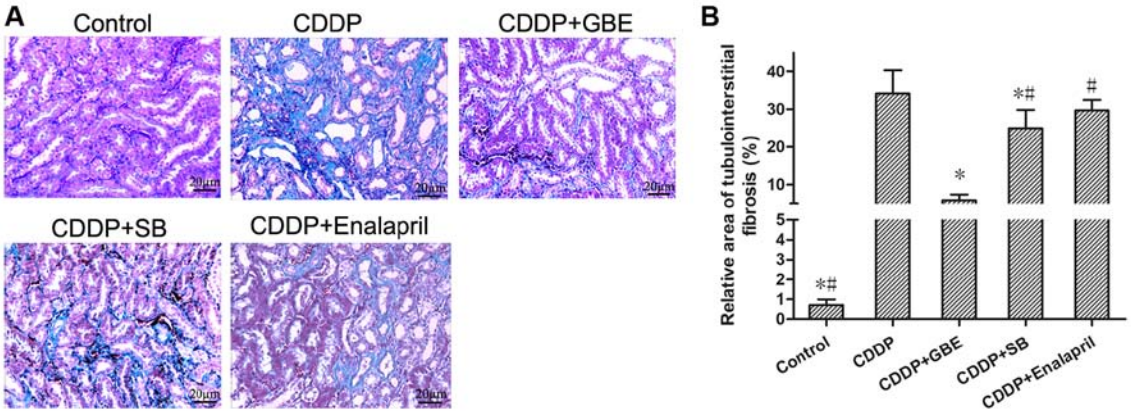

Figure 3. Effect of GBE on the degree of renal tubulointerstitial fibrosis was detected using Masson's trichrome staining. (A) Representative images of Masson's trichrome stained renal tissue samples. Magnification, x400. Blue stained areas are the collagen fibers, which is indicative of fibrosis, whereas the unaffected areas are stained purplish red. (B) Quantitative assessment of tubulointerstitial fibrosis. Data are presented as the mean ± standard deviation. n=9. *P<0.05 vs. CDDP group, #P<0.05 vs. CDDP + GBE group. GBE, Ginkgo biloba extract; SB, SB203580.

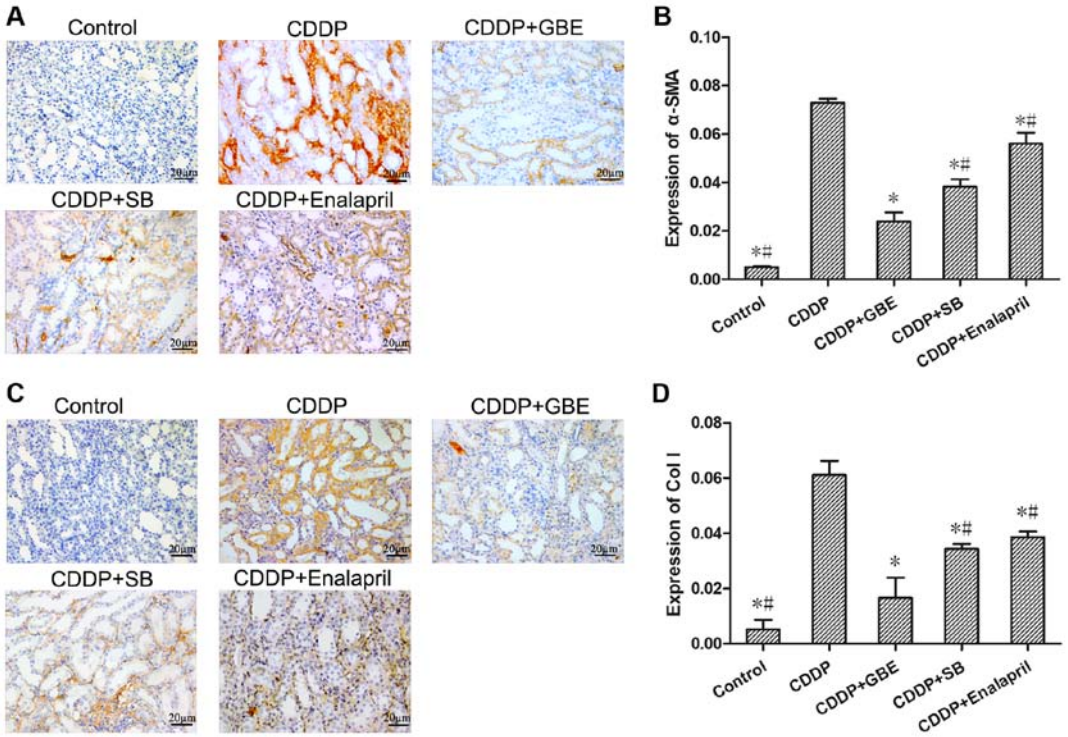

Figure 4. Effect of GBE on α-SMA and Col I expression in rat renal tissues. α-SMA and Col I levels were detected using immunohistochemical staining. (A and C) Representative images of immunohistochemically stained renal tissue sections. Magnification, x400. α-SMA and Col I proteins were primarily expressed in renal tubular epithelial cells. Quantitative analysis of the expression levels of α-SMA (B) and Col I (D) in renal tissues. Data are presented as the mean ± standard deviation. n=9. *P<0.05 vs. CDDP group, #P<0.05 vs. CDDP + GBE group. GBE, Ginkgo biloba extract; SB, SB203580; α-SMA, α-smooth muscle actin; Col I, collagen 1.

treatment resulted in a higher relative area of renal interstitial fibrosis compared with the control rats (P<0.05). The area of renal interstitial fibrosis induced by cisplatin was significantly reduced following treatment with GBE or SB (P<0.05), whereas enalapril had no notable effect (P>0.05). Additionally, The rats treated with GBE exhibited minimal areas of renal interstitial fibrosis compared with the rats treated with SB or enalapril (P<0.05; Fig. 3).

Effect of GBE on the protein expression levels of renal α-SMA and Col I in rats treated with cisplatin. As shown in Fig. 4, immunohistochemical staining showed that the expression of α-SMA and Col I in renal tubular tissues was very low in the control rats. Cisplatin increased the levels of α-SMA and Col I significantly (P<0.05). Additionally, GBE, SB or Enalapril treatment reduced the levels of α-SMA and Col I induced by cisplatin (P<0.05). The levels of α-SMA and Col I were higher in the SB treated rats compared with the GBE treated rats (P<0.05).

Effect of GBE on renal apoptosis in rats treated with cisplatin. TUNEL staining showed the proportion of apoptotic cells in the control rats was very low, and cisplatin significantly

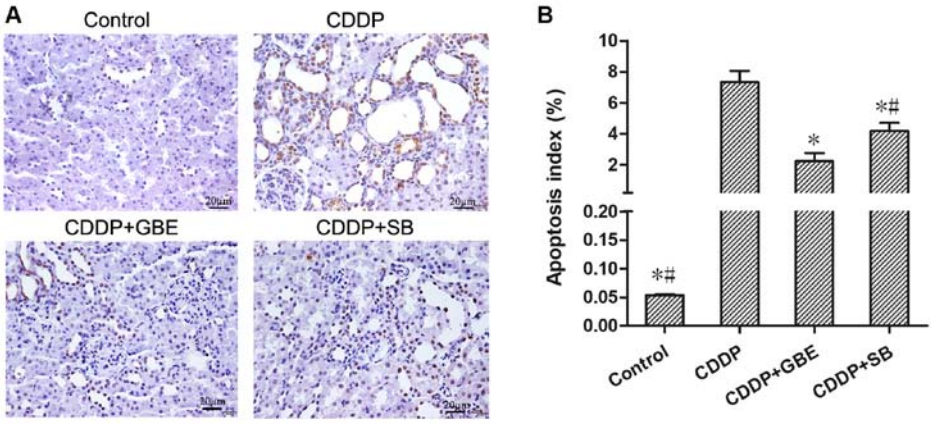

Figure 5. Effects of GBE on apoptosis of renal tissues was analyzed using TUNEL staining. (A) Representative images of TUNEL staining. Magnification, x400. Apoptotic cells were stained brown and normal cells appeared blue-purple. (B) Quantitative analysis of the TUNEL staining. Data are presented as the mean ± standard deviation. n=9. *P<0.05 vs. CDDP group, #P<0.05 vs. CDDP + GBE group. GBE, Ginkgo biloba extract; SB, SB203580.

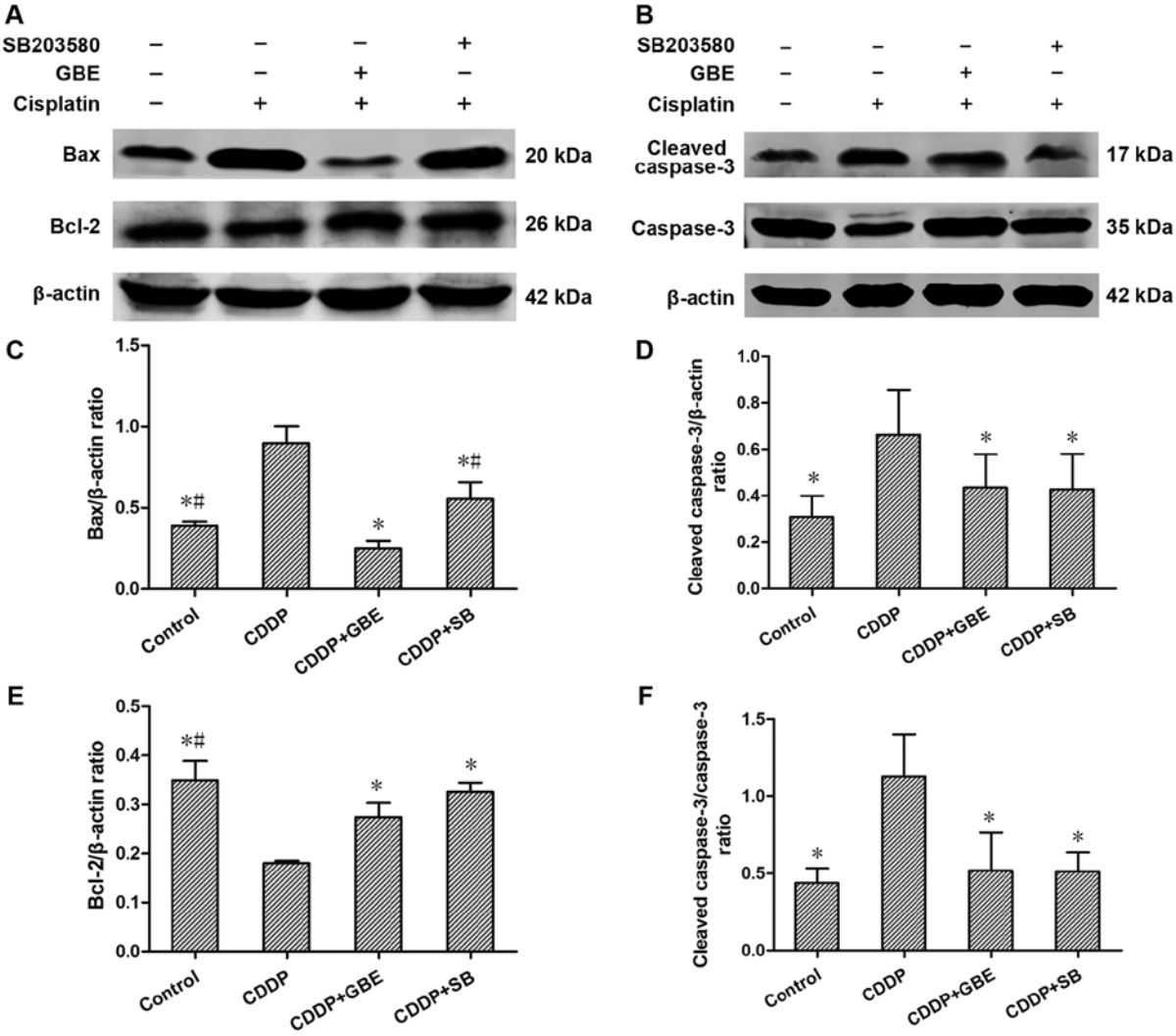

Figure 6. Effects of GBE on protein expression levels of Bcl-2, Bax, caspase-3 and cleaved caspase-3 in renal tissue. Protein expression levels were detected using western blotting. (A and B) Representative blots of apoptosis-associated proteins. (C-F) Densitometry analysis of the apoptosis-associated proteins. Data are presented as the mean ± standard deviation. n=9. *P<0.05 vs. CDDP group, #P<0.05 vs. CDDP + GBE group. GBE, Ginkgo biloba extract; SB, SB203580.

increased apoptosis (P<0.05). GBE and SB notably reduced the increase in apoptosis induced by cisplatin (P<0.05), and the effects of GBE were greater than that of SB (P<0.05; Fig. 5).

Effect of GBE on the protein expression levels of apoptosis associated proteins. Western blotting analysis indicated that compared with the control rats, Bax and cleaved

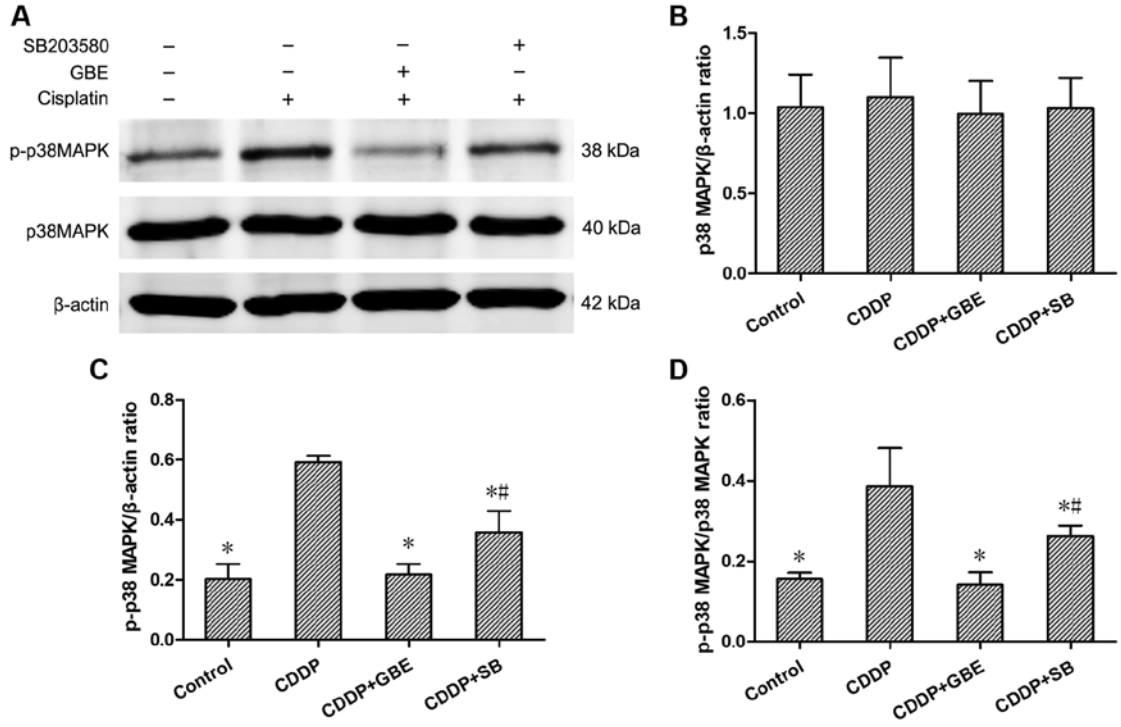

Figure 7. Effects of GBE on protein expression levels of p38MAPK and p-p38MAPK in renal tissues. Protein expression levels were measured using western blotting. (A) Representative blots of p38 and p-p38 expression. (B-D) Densitometry analysis of p38 and p-p38 expression. Data are presented as the mean ± standard deviation. n=9. *P<0.05 vs. CDDP group, #P<0.05 vs. CDDP + GBE group. GBE, Ginkgo biloba extract; SB, SB203580; p-, phospho-.

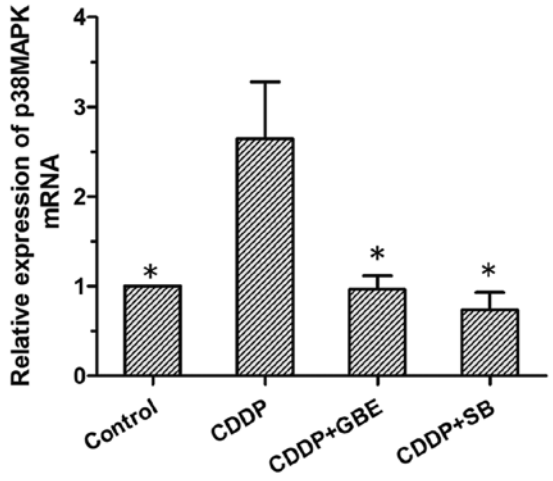

Figure 8. Effects of GBE on *p38MAPK* mRNA expression in renal tissues. RT-qPCR was used to detect p38MAPK mRNA expression. Data are presented as the mean ± standard deviation. n=9. *P<0.05 vs. CDDP group. GBE, Ginkgo biloba extract; SB, SB203580.

caspase-3 protein expression levels, as well as the cleaved caspase-3/caspase-3 ratio in rats treated with cisplatin were all markedly elevated (P<0.05). GBE and SB lowered the levels of Bax and cleaved caspase-3 levels, as well as the cleaved caspase-3/caspase-3 ratio induced by cisplatin significantly (P<0.05), and the effects of GBE were greater than that of SB (P<0.05; Fig. 6).

Conversely, Bcl-2 levels in the rats treated with cisplatin were reduced significantly compared with the control rats (P<0.05). GBE and SB increased Bcl-2 protein expression levels significantly (P<0.05; Fig. 6).

Effect of GBE on the protein expression levels of renal p38MAPK, p-p38MAPK and the phosphorylation ratio in rats treated with cisplatin. The expression levels of p38MAPK and p-p38MAPK were detected using western blotting. The results showed that the endogenously low expression of p-p38MAPK, as well as the low p-p38MAPK/p38MAPK ratio in control rats was increased following cisplatin treatment (P<0.05). Additionally, GBE and SB significantly decreased the p-p38MAPK levels and the p-p38MAPK/p38MAPK ratio compared with cisplatin treated rats (P<0.05). The effects of GBE were greater than that of SB in reducing p38MAPK levels (P<0.05; Fig. 7).

Effect of GBE on the levels of p38MAPK mRNA in rats treated with cisplatin. The results of RT-qPCR analysis showed that the p38MAPK mRNA expression levels were low in the control rats, and that cisplatin treatment alone significantly increased its levels (P<0.05). The levels of p38MAPK mRNA were significantly reduced following GBE or SB treatment. (P<0.05; Fig. 8).

Effect of GBE on the protein expression levels of renal TGF-β1 and HIF-1α in rats treated with cisplatin. As shown in Fig. 9, immunohistochemical analysis was used to measure TGF-β1 and HIF-1α levels. It could be seen that TGF-β1 and HIF-1α protein expression was concentrated in the epithelial cells of renal tubules. The TGF-β1 and HIF-1α levels in the cisplatin treated rats were significantly increased compared with the normal rats. Additionally, GBE and SB all significantly reduced TGF-β1 levels, as well as the HIF-1α levels induced by cisplatin (P<0.05). Moreover, the effect of GBE on lowering HIF-1α levels was greater than that of SB (P<0.05).

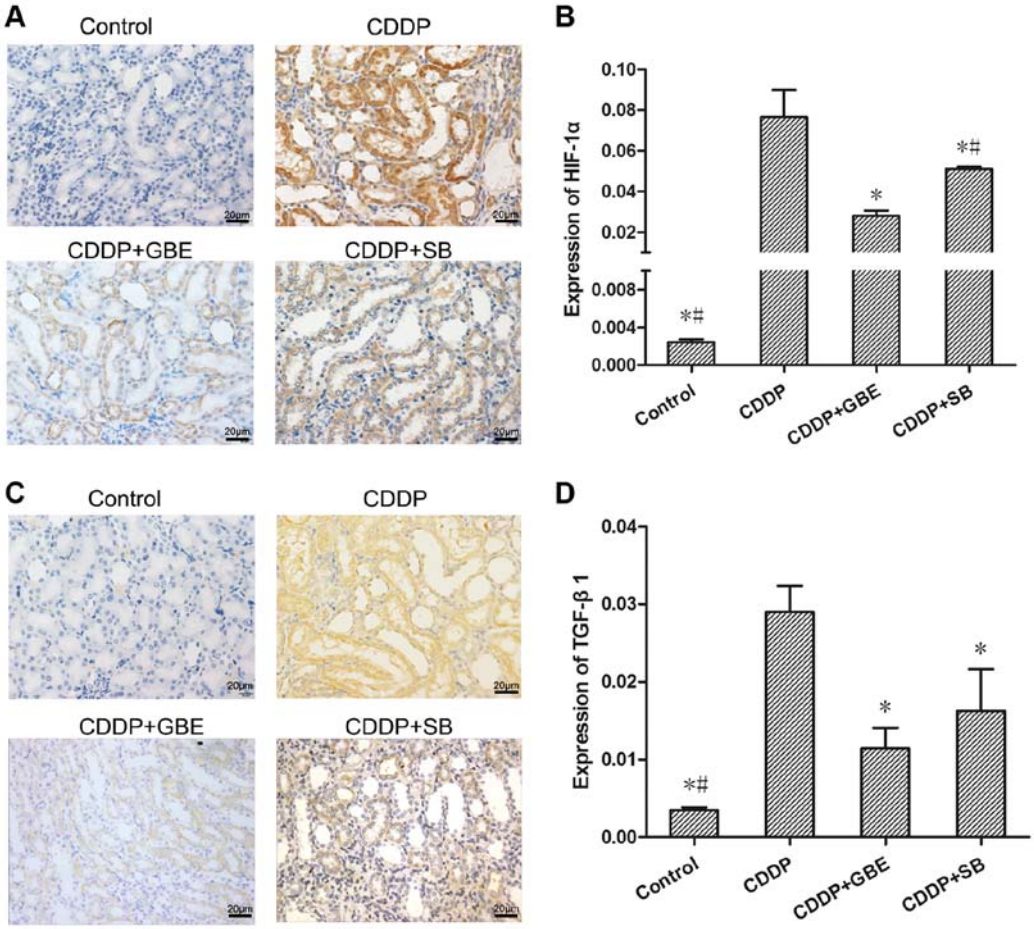

Figure 9. Effect of GBE on HIF-1α and TGF-β1 expression in rat renal tissues. The expression of HIF-1α and TGF-β1 was detected using immunohistochemical staining and quantified. (A and C) Representative images of immunohistochemically stained renal tissue sections. Magnification, x400. HIF-1α and TGF-β1 protein expression was primarily observed in the renal tubular epithelial cells. (B and D) Quantitative analysis of HIF-1α and TGF-β1 proteins expression levels in renal tissues, respectively. Data are presented as the mean ± standard deviation. n=9. *P<0.05 vs. CDDP group, $^{\#}$P<0.05 vs. CDDP + GBE group. GBE, Ginkgo biloba extract; SB, SB203580; HIF-1α, hypoxia inducible factor-1α.

Discussion

Cisplatin is a frequently-used chemotherapeutic option, and nephrotoxicity is a common adverse reaction (28). Our previous studies have shown that a single dose of cisplatin (converted from a single common clinical dose used in adults) can induce AKI in rats (10,11,29). Without intervention, AKI may develop into renal interstitial fibrosis (30,31). In the present study, the Scr, BUN and NAG levels were significantly increased in rats treated with a single dose of cisplatin. Additionally, the tubular injury score, renal interstitial fibrosis, and protein expression levels of α-SMA and Col I were all significantly increased, showing that cisplatin resulted in renal injury and interstitial fibrosis in rats. These results confirmed the successful establishment of a rat model of renal interstitial fibrosis induced by cisplatin, and suggested that cisplatin-induced renal interstitial fibrosis may be common in clinical applications.

The mechanism by which cisplatin induces renal interstitial fibrosis remains unclear, and there is a lack of effective treatment measures. According to previous studies, cell apoptosis and inflammatory damage are the primary mechanisms by which cisplatin induces AKI (32-34). Some traditional Chinese medicines, which possess anti-inflammatory or anti-apoptotic effects have been shown to protect against kidney injury induced by cisplatin (35,36). GBE is extracted from ginkgo biloba leaves, which is a traditional Chinese natural herb and has a long history of clinical use for treatment of cardiovascular and cerebrovascular diseases (37). Previously, GBE has been reported to ameliorate AKI in animal models induced by ischemia reperfusion (38,39) or by cisplatin (19,40). However, whether GBE can ameliorate renal interstitial fibrosis following cisplatin-induced AKI has not been assessed. The results of the present study showed that GBE significantly reduced the deterioration in renal function induced by cisplatin, reversed the increase in fibrosis related indicators, and reduced the degree of renal interstitial injury and fibrosis in rats. These findings suggest that GBE protected against renal function in rats and improved renal interstitial fibrosis induced by cisplatin. However, the molecular mechanisms underlying its anti-renal interstitial fibrosis effects have not been determined.

Several studies have shown that renal interstitial fibrosis is related to apoptosis of renal tubular epithelial cells and tubular damage (41,42). Apoptosis of renal tubular epithelial cells is a major mechanism underlying renal interstitial fibrosis and cisplatin-induced AKI (9,43). Cisplatin may induce apoptosis of renal tubular epithelial cells both *in vitro* and *in vivo* (44). Previously, it has been shown GBE inhibits

hepatocyte apoptosis and improves liver fibrosis by regulating the p38MAPK and Bcl-2/Bax pathways (45). In the present study, GBE significantly decreased cisplatin-induced apoptosis in rat renal tissues, decreased the levels of Bax and caspase-3, as well as the cleaved caspase-3/caspase-3 ratio, and increased Bcl-2 protein expression. These results suggest that GBE attenuated cisplatin-induced renal interstitial fibrosis via inhibition of apoptosis.

p38 MAPK is closely related to apoptosis and serves a key role in this process (46). The activation of p38 MAPK (p-p38 MAPK) mediated chemotherapeutic drug-induced apoptosis (47), and administration of a p38 MAPK inhibitor completely abolished TGF-β1 levels and inhibited fibrosis in human mesangial cells (48). The p38 MAPK/TGF-β1 pathway was shown to mediate oxidative damage and promoted fibrosis of the liver (49). Additionally, HIF-1α inhibition attenuated hypoxia-induced apoptosis of renal tubular cells (50), and elevated levels of HIF-1α may aggravate tissue fibrosis (51). Our previous study found that HIF-1α was elevated in rat kidneys, which had a protective effect on cisplatin-induced AKI (11). Importantly, GBE improved liver fibrosis by inhibiting the apoptosis of hepatic stellate cells via the p38 MAPK pathway (16), and prevented rats from CCl4-induced liver fibrosis by inhibiting TGF-β1 (52). GBE also regulated the expression of HIF-1α mRNA and protein expression induced by hypoxia or ischemic stroke (53,54). A previous study demonstrated that GBE prevented renal fibrosis in rats with diabetic nephropathy (24), which likely result3ed in reduced formation of glomerular lesions. This suggests that GBE improved tissue fibrosis via inhibition of apoptosis, by regulation of p38 MAPK, TGF-β1 and HIF-1α. In the present study, p38 MAPK mRNA expression levels, and the protein expression levels of p-p38 MAPK, TGF-β1 and HIF-1α were significantly increased, and this was accompanied by an increase in the rate of apoptosis and apoptosis-related proteins, and decreased expression of Bcl-2 in renal tissues exposed to cisplatin. Furthermore, GBE significantly reversed the effects of cisplatin on these indicators of apoptosis, and this was accompanied by a decrease in the apoptotic rate and in the expression of apoptosis-related proteins. These findings suggest that GBE improved cisplatin-induced renal interstitial fibrosis via reduction of renal apoptosis and inhibition of p38 MAPK, TGF-β1 and HIF-1α function.

It is worth noting that the specific p38MAPK inhibitor SB significantly reversed all cisplatin-induced effects on indicators of renal function, renal tissue injury and fibrosis. These results confirm that p38MAPK is involved in promoting renal interstitial fibrosis in cisplatin-induced AKI. Additionally, SB also significantly reversed the rate of renal tissue apoptosis and the changes in the expression of apoptosis-associated proteins induced by cisplatin, and these results confirm that p38MAPK promoted renal interstitial fibrosis following cisplatin-induced AKI by increasing renal tissue apoptosis. Moreover, SB also significantly reversed cisplatin-induced changes in expression of p38 MAPK, TGF-β1 and HIF-1α, and these results confirm that p38MAPK promoted the expression of TGF-β1 and HIF-1α. The above results indicate that GBE improved renal interstitial fibrosis following cisplatin-induced AKI by inhibiting apoptosis via the p38 MAPK/TGF-β1 and p38 MAPK/HIF-1α pathways.

Although SB functions in a similar manner to GBE, GBE was significantly more effective than SB in reducing p-P38 MAPK, TGF-β1 and HIF-1α protein expression levels, as well as renal apoptosis, injury and fibrosis. This may be due to the fact that GBE contains multiple active ingredients (55), and several of these may exhibit anti-fibrotic effects via different pathways, including quercetin and kaempferol (56,57). Kaempferoll exhibits an inhibitory effect on TGF-β1-induced fibrosis related genes in renal tubular epithelial cells, and improves renal function in rats (58). Therefore, in addition to p38MAPK, GBE may inhibit TGF-β1 and HIF-1α through other pathways, thereby inhibiting apoptosis and fibrosis, and this may explain the improved effectiveness of GBE compared with SB, and highlights a key advantage of Traditional Chinese Medicines.

In conclusion, the present study is the first to show that GBE could effectively ameliorate renal interstitial fibrosis following cisplatin-induced AKI by inhibiting renal apoptosis, and this was mediated by downregulation of the p38MAPK/TGF-β1 and p38MAPK/HIF-1α signaling pathways.

Acknowledgements

Not applicable.

Funding

The present study was supported by funding from China's National Natural Science Foundation (grant nos. 82060801, 81560729 and 81260598), the Natural Science Foundation of Guangxi (grant nos. 2017GXNSFAA198262 and 2018GXNSFAA294043), and a self-funded project from the Health Commission of Guangxi Zhuang Autonomous Region (grant no. Z20200180).

Availability of data and materials

The datasets used and/or analyzed during the present study are available from the corresponding author on reasonable request.

Authors' contributions

TL, CW and SL performed the experiments. MQ, GQ, YZ and XZhong performed the statistical analysis. XZou assisted in the design of the study. YY conceived and designed the study, and wrote the manuscript. All authors read and approved the final manuscript.

Ethics approval and consent to participate

The present study was approved by the Ethics Committee of Guangxi Medical University (approval no. 201310009) (Nanning, China).

Patient consent for publication

Not applicable.

Competing interests

The authors declare that they have no competing interests.

Referencess

1. Dasari S and Tchounwou PB: Cisplatin in cancer therapy: Molecular mechanisms of action. Eur J Pharmacol 740: 364-378, 2014.
2. Parr SK and Siew ED: Delayed consequences of acute kidney injury. Adv Chronic Kidney Dis 23: 186-194, 2016.
3. Yu CC, Chien CT and Chang TC: M2 macrophage polarization modulates epithelial-mesenchymal transition in cisplatin-induced tubulointerstitial fibrosis. Biomedicine (Taipei) 6: 5, 2016.
4. Qi W, Chen X, Poronnik P and Pollock CA: The renal cortical fibroblast in renal tubulointerstitial fibrosis. Int J Biochem Cell Biol 38: 1-5, 2006.
5. El-Naga RN: Pre-treatment with cardamonin protects against cisplatin-induced nephrotoxicity in rats: Impact on NOX-1, inflammation and apoptosis. Toxicol Appl Pharmacol 274: 87-95, 2014.
6. Qi ZL, Wang Z, Li W, Hou JG, Liu Y, Li XD, Li HP and Wang YP: Nephroprotective effects of anthocyanin from the fruits of Panax ginseng (GFA) on Cisplatin-induced acute kidney injury in mice. Phytother Res 31: 1400-1409, 2017.
7. Nangaku M, Rosenberger C, Heyman SN and Eckardt KU: Regulation of hypoxia-inducible factor in kidney disease. Clin Exp Pharmacol Physiol 40: 148-157, 2013.
8. Kim IH, Kwon MJ, Jung JH and Nam TJ: Protein extracted from Porphyra yezoensis prevents cisplatin-induced nephrotoxicity by downregulating the MAPK and NF-κB pathways. Int J Mol Med 41: 511-520, 2018.
9. Thongnuanjan P, Soodvilai S, Chatsudthipong V and Soodvilai S: Fenofibrate reduces cisplatin-induced apoptosis of renal proximal tubular cells via inhibition of JNK and p38 pathways. J Toxicol Sci 41: 339-349, 2016.
10. Liang X, Yang Y, Huang Z, Zhou J, Li Y and Zhong X: Panax notoginseng saponins mitigate cisplatin induced nephrotoxicity by inducing mitophagy via HIF-1α. Oncotarget 8: 102989-103003, 2017.
11. Liu X, Huang Z, Zou X, Yang Y, Qiu Y and Wen Y: Possible mechanism of PNS protection against cisplatin-induced nephrotoxicity in rat models. Toxicol Mech Methods 25: 347-354, 2015.
12. Li X, Lu L, Chen J, Zhang C, Chen H and Huang H: New Insight into the mechanisms of ginkgo Biloba extract in vascular aging prevention. Curr Vasc Pharmacol 18: 334-345, 2020.
13. EGb 761: Ginkgo biloba extract, Ginkor. Drugs R D 4: 188-193, 2003.
14. Gevrek F, Biçer Ç, Kara M and Erdemir F: The ameliorative effects of Ginkgo biloba on apoptosis, LH-R expression and sperm morphology anomaly in testicular torsion and detorsion. Andrologia: Feb 7, 2018 (Epub ahead of print).
15. Wang A, Yang Q, Li Q, Wang X, Hao S, Wang J and Ren M: Ginkgo Biloba L. Extract reduces H2O2-induced bone marrow mesenchymal stem cells cytotoxicity by regulating mitogen-activated protein kinase (MAPK) signaling pathways and oxidative stress. Med Sci Monit 24: 3159-3167, 2018.
16. Wang R, Zhang H, Wang Y, Song F and Yuan Y: Inhibitory effects of quercetin on the progression of liver fibrosis through the regulation of NF-κB/IκBα, p38 MAPK, and Bcl-2/Bax signaling. Int Immunopharmacol 47: 126-133, 2017.
17. Li Y, Xiong Y, Zhang H, Li J, Wang D, Chen W, Yuan X, Su Q, Li W, Huang H, *et al*: Ginkgo biloba extract GBE761 attenuates brain death-induced renal injury by inhibiting pro-inflammatory cytokines and the SAPK and JAK-STAT signalings. Sci Rep 7: 45192, 2017.
18. Cao CJ, Su Y, Sun J, Wang GY, Jia XQ, Chen HS and Xu AH: Anti-tumor effect of ginkgo biloba exocarp extracts on B16 melanoma bearing mice involving P I3K/Akt/HIF-1α/VEGF signaling pathways. Iran J Pharm Res 18: 803-811, 2019.
19. Yang YF, Lao S, Luo M and Zeng J: Dynamic observation of the protective effect of ginkgo biloba extract on cisplatin kidney damage in rabbits. Lishizhen Medicine and Materia Medica 22: 2897-2898, 2011.
20. Wei W, Wu XM and Li YJ: Experimental Methodology of Pharmacology. 4th edition. People's Medical Publishing House, Beijing, pp1439-1442, 2010.
21. Asaad GF, Hassan A and Mostafa RE: Anti-oxidant impact of Lisinopril and Enalapril against acute kidney injury induced by doxorubicin in male Wistar rats: Involvement of kidney injury molecule-1. Heliyon 7: e05985, 2021.
22. Sun N, Zhai L, Li H, Shi LH, Yao Z and Zhang B: Angiotensin-converting enzyme inhibitor (ACEI)-mediated amelioration in renal fibrosis involves suppression of mast cell degranulation. Kidney Blood Press Res 41: 108-118, 2016.
23. Ražná K, Sawinska Z, Ivanišová E, Vukovic N, Terentjeva M, Stričík M, Kowalczewski PŁ, Hlavačková L, Rovná K, Žiarovská J and Kačániová M: Properties of *Ginkgo biloba* L.: Antioxidant characterization, antimicrobial activities, and genomic MicroRNA based marker fingerprints. Int J Mol Sci 21: 3087, 2020.
24. Lu Q, Zuo WZ, Ji XJ, Zhou YX, Liu YQ, Yao XQ, Zhou XY, Liu YW, Zhang F and Yin XX: Ethanolic Ginkgo biloba leaf extract prevents renal fibrosis through Akt/mTOR signaling in diabetic nephropathy. Phytomedicine 22: 1071-1078, 2015.
25. Yang H, Zhang W, Xie T, Wang X and Ning W: Fluorofenidone inhibits apoptosis of renal tubular epithelial cells in rats with renal interstitial fibrosis. Braz J Med Biol Res 52: e8772, 2019.
26. Li A, Zhang X, Shu M, Wu M, Wang J, Zhang J, Wang R, Li P and Wang Y: Arctigenin suppresses renal interstitial fibrosis in a rat model of obstructive nephropathy. Phytomedicine 30: 28-41, 2017.
27. Yuan JS, Reed A, Chen F and Stewart CN Jr: Statistical analysis of real-time PCR data. BMC Bioinformatics 7: 85, 2006.
28. Yamamoto Y, Watanabe K, Tsukiyama I, Matsushita H, Yabushita H, Matsuura K and Wakatsuki A: Nephroprotective effects of hydration with magnesium in patients with cervical cancer receiving cisplatin. Anticancer Res 35: 2199-2204, 2015.
29. Li Q, Liang X, Yang Y, Zeng X, Zhong X and Huang C: Panax notoginseng saponins ameliorate cisplatin-induced mitochondrial injury via the HIF-1α/mitochondria/ROS pathway. FEBS Open Bio 10: 118-126, 2020.
30. Lu S, Zhong X, Yang Y, Zou X, Liang X and Cai G: Effects of single dose of cisplatin on renal interstitial fibrosis indicators in rats. China Pharmacy 29: 298-302, 2018.
31. Johnson FL, Patel NSA, Purvis GSD, Chiazza F, Chen J, Sordi R, Hache G, Merezhko VV, Collino M, Yaqoob MM and Thiemermann C: Inhibition of IκB kinase at 24 hours after acute kidney injury improves recovery of renal function and attenuates fibrosis. J Am Heart Assoc 6: e005092, 2017.
32. Ozkok A and Edelstein CL: Pathophysiology of cisplatin-induced acute kidney injury. Biomed Res Int 2014: 967826, 2014.
33. Pabla N and Dong Z: Cisplatin nephrotoxicity: Mechanisms and renoprotective strategies. Kidney Int 73: 994-1007, 2008.
34. Pabla N and Dong Z: Curtailing side effects in chemotherapy: A tale of PKCδ in cisplatin treatment. Oncotarget 3: 107-111, 2012.
35. Huang SJ, Huang J, Yan YB, Qiu J, Tan RQ, Liu Y, Tian Q, Guan L, Niu SS, Zhang Y, *et al*: The renoprotective effect of curcumin against cisplatin-induced acute kidney injury in mice: Involvement of miR-181a/PTEN axis. Ren Fail 42: 350-357, 2020.
36. Lee IC, Ko JW, Park SH, Shin NR, Shin IS, Kim YB and Kim JC: Ameliorative effects of pine bark extract on cisplatin-induced acute kidney injury in rats. Ren Fail 39: 363-371, 2017.
37. Tian J, Liu Y and Chen K: Ginkgo biloba extract in vascular protection: Molecular mechanisms and clinical applications. Curr Vasc Pharmacol 15: 532-548, 2017.
38. Wang Y, Pei DS, Ji HX and Xing SH: Protective effect of a standardized Ginkgo extract (ginaton) on renal ischemia/reperfusion injury via suppressing the activation of JNK signal pathway. Phytomedicine 15: 923-931 2008.
39. Sener G, Sener E, Sehirli O, Oğünç AV, Cetinel S, Gedik N and Sakarcan A: Ginkgo biloba extract ameliorates ischemia reperfusion-induced renal injury in rats. Pharmacol Res 52: 216-222, 2005.
40. Gulec M, Iraz M, Yilmaz HR, Ozyurt H and Temel I: The effects of ginkgo biloba extract on tissue adenosine deaminase, xanthine oxidase, myeloperoxidase, malondialdehyde, and nitric oxide in cisplatin-induced nephrotoxicity. Toxicol Ind Health 22: 125-130, 2006.
41. Younis NN, Elsherbiny NM, Shaheen MA and Elseweidy MM: Modulation of NADPH oxidase and Nrf2/HO-1 pathway by vanillin in cisplatin-induced nephrotoxicity in rats. J Pharm Pharmacol 72: 1546-1555, 2020.
42. Jing Z, Hu L, Su Y, Ying G, Ma C and Wei J: Potential signaling pathway through which Notch regulates oxidative damage and apoptosis in renal tubular epithelial cells induced by high glucose. J Recept Signal Transduct Res: Sep 16, 2020 (Epub ahead of print).
43. Zhang XF, Yang Y, Zhang J and Cao W: Microvesicle-containing miRNA-153-3p induces the apoptosis of proximal tubular epithelial cells and participates in renal interstitial fibrosis. Eur Rev Med Pharmacol Sci 23: 10065-10071, 2019.
44. Du B, Dai XM, Li S, Qi GL, Cao GX, Zhong Y, Yin PD and Yang XS: MiR-30c regulates cisplatin-induced apoptosis of renal tubular epithelial cells by targeting Bnip3L and Hspa5. Cell Death Dis 8: e2987, 2017.

45. Wang Y, Wang R, Wang Y, Peng R, Wu Y and Yuan Y: Ginkgo biloba extract mitigates liver fibrosis and apoptosis by regulating p38 MAPK, NF-κB/IκBα, and Bcl-2/Bax signaling. Drug Des Devel Ther 9: 6303-6317, 2015.
46. Cuadrado A and Nebreda AR: Mechanisms and functions of p38 MAPK signalling. Biochem J 429: 403-417, 2010.
47. Deacon K, Mistry P, Chernoff J, Blank JL and Patel R: p38 Mitogen-activated protein kinase mediates cell death and p21-activated kinase mediates cell survival during chemotherapeutic drug-induced mitotic arrest. Mol Biol Cell 14: 2071-2087, 2003.
48. Liu Z, Xue L, Liu Z, Huang J, Wen J, Hu J, Bo L and Yang R: Tumor necrosis factor-like weak inducer of apoptosis accelerates the progression of renal fibrosis in lupus nephritis by activating SMAD and p38 MAPK in TGF-β1 signaling pathway. Mediators Inflamm 2016: 8986451, 2016.
49. Li ZL, Shi Y, Le G, Ding Y and Zhao Q: 24-week exposure to oxidized tyrosine induces hepatic fibrosis involving activation of the MAPK/TGF-β1 signaling pathway in Sprague-Dawley Rats model. Oxid Med Cell Longev 2016: 3123294, 2016.
50. Liu LL, Li D, He YL, Zhou YZ, Gong SH, Wu LY, Zhao YQ, Huang X, Zhao T, Xu L, *et al*: MiR-210 protects renal cell against hypoxia-induced apoptosis by targeting HIF-1alpha. Mol Med 23: 258-271, 2017.
51. Liu L, Zhang P, Bai M, He L, Zhang L, Liu T, Yang Z, Duan M, Liu M, Liu B, *et al*: p53 upregulated by HIF-1α promotes hypoxia-induced G2/M arrest and renal fibrosis in vitro and in vivo. J Mol Cell Biol 11: 371-382, 2019.
52. Liu SQ, Yu JP, Chen HL, Luo HS, Chen SM and Yu HG: Therapeutic effects and molecular mechanisms of ginkgo biloba extract on liver fibrosis in rats. Am J Chin Med 34: 99-114, 2006.
53. Oh JH, Oh J, Togloom A, Kim SW and Huh K: Effects of ginkgo biloba extract on cultured human retinal pigment epithelial cells under chemical hypoxia. Curr Eye Res 38: 1072-1082, 2013.
54. Chen M, Zou W, Chen M, Cao L, Ding J, Xiao W and Hu G: Ginkgolide K promotes angiogenesis in a middle cerebral artery occlusion mouse model via activating JAK2/STAT3 pathway. Eur J Pharmacol 833: 221-229, 2018.
55. Singh B, Kaur P, Gopichand, Singh RD and Ahuja PS: Biology and chemistry of Ginkgo biloba. Fitoterapia 79: 401-418, 2008.
56. Wang T, Xiao J, Hou H, Li P, Yuan Z, Xu H, Liu R, Li Q and Bi K: Development of an ultra-fast liquid chromatography-tandem mass spectrometry method for simultaneous determination of seven flavonoids in rat plasma: Application to a comparative pharmacokinetic investigation of Ginkgo biloba extract and single pure ginkgo flavonoids after oral administration. J Chromatogr B Analyt Technol Biomed Life Sci 1060: 173-181, 2017.
57. Ji X, Cao J, Zhang L, Zhang Z, Shuai W and Yin W: Kaempferol protects renal fibrosis through activating the BMP-7-Smad1/5 signaling pathway. Biol Pharm Bull 43: 533-539, 2020.
58. Liu X, Sun N, Mo N, Lu S, Song E, Ren C and Li Z: Quercetin inhibits kidney fifibrosis and the epithelial to mesenchymal transition of the renal tubular system involving suppression of the Sonic Hedgehog signaling pathway. Food Funct 10: 3782-3797, 2019.